

# Simulation of Vortex-Antivortex Pair Production in a Phase Transition with Explicit Symmetry Breaking

Sanatan Digal, Supratim Sengupta and Ajit M. Srivastava \*

*Institute of Physics*

*Sachivalaya Marg, Bhubaneswar-751005, INDIA*

We carry out numerical simulation of the formation of U(1) global vortices in a first order phase transition in 2+1 dimensions in the presence of small explicit symmetry breaking. Bubbles of broken symmetry phase are randomly nucleated, which grow and coalesce. Vortices form at junctions of bubbles via standard Kibble mechanism as well as due to a new mechanism, recently proposed by us, where defect-antidefect pairs are produced due to field oscillations. In a simulation involving nucleation of 63 bubbles, with bias in phase distribution inside bubbles arising from explicit symmetry breaking, we find that not a single vortex/antivortex is produced via the Kibble mechanism, while the new mechanism leads to production of 104 vortices and antivortices. Even without biasing the phase distribution inside bubbles, the vortex production is completely dominated by this new mechanism, which accounts for the production of about 80% of the vortices and antivortices, remaining 20% being produced via the Kibble mechanism. We study the dependence of the effectiveness of the new mechanism on the magnitude of explicit symmetry breaking, as well as on the nucleation rate of bubbles. We also study the effect of damping on this mechanism and show that damping suppresses this mode of vortex production.

PACS numbers: 98.80.Cq, 61.30.Jf, 12.39.Dc

## I. INTRODUCTION

There has been a renewed interest recently in studying the formation of topological defects in phase transitions. It is clearly important to understand various processes which could be responsible for defect formation as then only one can hope to get a true understanding of the distribution of defects and its time evolution. These issues are of great importance not only for condensed matter physics but also in the context of particle physics models of the early Universe where topological defects are supposed to play an important role in the evolution of the Universe and in the structure formation [1].

In conventional studies only two distinct types of processes have been considered to be important in studying the formation of topological defects in phase transitions. One of these is based on thermal production of defects which leads to defect density which is suppressed by the Boltzmann factor [2]. The other process is based on the formation of a kind of domain structure during phase transition with defects forming at the junctions of these domains, and is typically known as the Kibble mechanism [3]. Kibble mechanism was originally proposed for studying defect formation in the early Universe. However, the mechanism as such has complete general applicability and in fact has been recently verified by study-

ing defect formation in certain condensed matter systems [4,5]. [Though, there are nontrivial issues for the case when gauge fields are also present. See ref. [6] and references therein.]

An important aspect of the Kibble mechanism is that it does not crucially depend on the dynamical details of the phase transition. For example, the number of defects (per domain) produced via the Kibble mechanism depends only on the topology of the order parameter space and on spatial dimensions. Dynamics plays a role here only in determining the relevant correlation length, which in turn determines the domain size, affecting net number of defects produced in a given region. Still, the number of defects per domain is entirely independent of the dynamics. [Apart from some special situations, e.g. in a very slow first order transition, see [7].]

Recently, a new mechanism for defect production has been proposed by us [8–10] where the dynamics of the order parameter field plays a very important role. Here, defect-antidefect pairs are produced due to strong oscillations of the field. We showed that whenever the field passes through zero magnitude, while oscillating, (in a region where the field is non-uniform), a defect-antidefect pair gets created. This essentially explains why the dynamics plays a major role in this mechanism since the nature and the strength of field oscillations during a phase

---

\*E-mail :

digal@iopb.stpbh.soft.net

supratim@iopb.stpbh.soft.net

ajit@iopb.stpbh.soft.net

transition will in general depend on various dynamical details, such as the order of the transition, time duration of the quench etc. We find that the number of defects (say per domain) produced via this mechanism can vary strongly as different parameters of the transition are changed.

This mechanism was first proposed by two of us [8] for systems in the presence of small explicit symmetry breaking. Using numerical simulation of two bubble collisions in 2+1 dimensions for the case of U(1) global vortices, it was shown in ref. [8] that a very large number of vortex-antivortex pairs can be created via this mechanism due to field oscillations enhanced by the explicit symmetry breaking. For example, in one case it was found that ten, well separated, vortices and antivortices were created in a single two bubble collision. It was later shown by us in ref. [9], that this mechanism was not restricted only to systems with explicit symmetry breaking, and is in fact very general. It applies even when there is no explicit symmetry breaking and is applicable to all sorts of topological defects. We also argued that this mechanism should be operative even in a second order phase transition involving quenching from a sufficiently high temperature. However, as this mechanism depends sensitively on dynamics, we found that defect production for the case of zero explicit symmetry breaking was not very prominent compared to the case with explicit symmetry breaking studied in ref. [8]. [At least for the range of bubble separations considered in ref. [8,9].]

Here we mention the work of Copeland and Saffin [6,11] who have considered the production of strings in gauge theories. They showed in ref. [6], for Abelian Higgs model, that the geodesic rule may get violated in the collision of two bubbles and that vortex-antivortex pairs can form in the region of coalescence. In their case also the oscillations of field played crucial role, though due to the presence of gauge field the dynamics of the phase  $\theta$  had extra features. For example, the presence of gauge fields provides a driving force for  $\theta$ . The dynamics of vortex production in ref. [6] is, in this sense, similar to the case of explicit symmetry breaking discussed in ref. [8].

The studies in ref. [8,9] were carried out by choosing specific initial bubble configurations. In order to study this mechanism in a realistic situation of a phase transition, we carried out a full study of the effectiveness of this mechanism, for the case of zero explicit symmetry breaking, by simulating a first order transition via random nucleation of bubbles [10]. We showed there that for very low bubble nucleation rates (leading to large inter-bubble separation and hence very energetic collisions), the new mechanism becomes the dominant mode of production of well separated vortices. However, for large nucleation rates the vortex-antivortex pairs produced via this mechanism consist of strongly overlapping field configurations which decay rapidly. Thus for large nucleation rates, number of surviving vortices will be roughly the same as expected from the Kibble mechanism. These results are

important as they show that defect production in certain situations (i.e. very low nucleation rate) may be drastically altered due to contributions of this mechanism. For example, this mechanism may completely dominate the production of cosmic strings, monopoles etc. in models of extended inflation in the early Universe, and may play an important role in the production of vortices in superfluid  $^3\text{He}$  A - B transition [12].

From the results in ref. [8] we expect that there is a special class of systems, those with small explicit symmetry breaking, where this mechanism may be remarkably effective in defect production during a phase transition. There are many examples of systems with spontaneously broken symmetries where the symmetry is also broken explicitly. In the context of particle physics, the Skyrmion picture of baryons in the context of chiral models is an example where explicit symmetry breaking terms are needed to incorporate a non-zero pion mass. In fact it was this system where the role of explicit symmetry breaking in enhancing defect production was first discussed by Kapusta and one of the author [13], though the underlying mechanism was different there. There is another example, in Particle physics, that of axionic strings arising from the breaking of the Pecci-Quinn symmetry, where explicit symmetry breaking is present [14]. It was suggested in [8–10] that this new mechanism may be especially effective for the production of axionic strings due to the presence of explicit symmetry breaking. However, that argument does not seem to be correct since the scale of Pecci-Quinn symmetry breaking is very large (of order  $10^{10}$  GeV or so) compared to the scale of explicit symmetry breaking, which arises at the QCD scale. Thus, at the Pecci-Quinn scale, explicit symmetry breaking can not play any role in the production of axionic strings, though this new mechanism may certainly contribute to their production.

In condensed matter, nematic liquid crystals provide a simple example of such systems where the presence of external electric or magnetic fields induces explicit symmetry breaking terms [15]. Hence this new mechanism may play a dominant role there. Though there are subtleties in considering this system due to the fact that opposite orientations of the order parameter are identified. We will discuss this point later in Section V.

From the point of view of these systems, and in general for systems with explicit symmetry breaking, it is important to know the actual contribution of this mechanism in a realistic phase transition. The study in ref. [8] considered some specific bubble configurations and showed how a very large number of defects may be produced in a single two bubble collision. What one needs to know is the average number of defects produced via this mechanism when bubbles are randomly nucleated. We have already carried out such a study for the case of zero explicit symmetry breaking, which is the case of widest possible applications. [For example, the production of cosmic strings, magnetic monopoles etc., in the early Universe, and the production of vortices in superfluid  $^3\text{He}$  and  $^4\text{He}$  in the

laboratory.] As the detailed dynamics, and hence the defect production via this mechanism, is very different for the systems with explicit symmetry breaking, we need to carry out detailed simulations of the phase transition for this case as well. Certainly, for baryon (Skyrmion) production in the heavy-ion collisions, as well as for the production of liquid crystal strings in the presence of external fields, the results of ref. [10] (for the zero symmetry breaking case) are not much useful. We should expect that a much more dramatic role will be played by the new mechanism for these systems, even in the generic situation of a phase transition.

There is one more reason why this mechanism may be most dominant in the situation with explicit symmetry breaking. If bubble nucleation is not happening at very large temperatures (compared to the explicit symmetry breaking scale) then the distribution of phases inside different bubbles will get biased. This bias will suppress vortex production due to Kibble mechanism. For example, in our simulation with 63 bubbles (discussed in Section IV), essentially all the bubbles had  $\theta$  which was either less than  $\pi/2$  or greater than  $3\pi/2$  (for the case when  $\theta = 0$  corresponds to the true vacuum). Due to this, not a single vortex was produced via the Kibble mechanism. Bias in  $\theta$  towards value zero does have adverse effect even on the new mechanism due to reduced potential energy which affects the flipping of the field. However, wall oscillations will be expected to be much larger now due to smaller  $\theta$  gradients between colliding bubbles. This should help vortex production via the new mechanism. What we find is that all the vortices and antivortices (a total of 104 in this case) were produced via the new mechanism. This is about the same average vortex production per bubble via the new mechanism as we obtain when  $\theta$  distribution inside bubbles is chosen to be uniform (though in that case there are some vortices produced via the Kibble mechanism as well).

We also would like to know how this average defect production is affected by dynamical details, such as the magnitude of explicit symmetry breaking, nucleation rate, presence of damping etc. We carry out a complete study of all these issues in this paper. We find that defect production increases with increasing magnitude of explicit symmetry breaking. Defect production also increases for lower nucleation rates due to bubble collisions being more energetic. This is the same behavior which was observed in ref. [10] for the case of zero explicit symmetry breaking. Presence of damping suppresses field oscillations and hence results in lower number of defects. However, compared to the case of zero explicit symmetry breaking discussed in ref. [10] where strong damping makes this mechanism completely ineffective, for the present case we find that some pairs are always produced via this mechanism (as long as explicit symmetry breaking is not too small). This results is very significant for the cases of experimental interest. For example, in the case of Skyrmion production in heavy-ion collisions, dissipative effects will always be present in the expanding plasma. This is es-

pecially true for the case of liquid crystal strings where the dynamics is completely dominated by dissipation.

The paper is organized in the following manner. The second section reviews the essential physical picture of the new mechanism [9] and discusses the numerical technique. Section III discusses the results of the simulation of the phase transition by random nucleation of bubbles with unbiased  $\theta$  distribution inside bubbles. In Section IV we present results for simulation with  $\theta$  distribution inside bubbles being biased according to the explicit symmetry breaking term. The dependence of vortex production on nucleation rate and the magnitude of explicit symmetry breaking is discussed in Section V. The effect of damping on this mechanism is discussed in Section VI and conclusions are presented in Section VII.

## II. PHYSICAL PICTURE OF THE MECHANISM AND NUMERICAL TECHNIQUE

We first briefly recall the essential features of this mechanism [9]. Consider the case of spontaneous breaking of a global U(1) symmetry, with the order parameter being the vacuum expectation value of a complex scalar field  $\Phi$ . The vacuum manifold is a circle  $S^1$ . After the phase transition,  $\Phi$  will have a non-zero magnitude but its phase  $\theta$  may vary spatially. Consider a region of space where  $\theta$  has some small variation between two points A and B. Now suppose that the magnitude of the field undergoes strong oscillations in a small region between points A and B. If  $\Phi$  passes through zero magnitude while oscillating in a region, then it is easy to see that  $\theta$  in that region will discontinuously change to  $\theta + \pi$ . We call it the flipping of  $\Phi$ . By drawing the distribution of  $\theta$ , with flipped orientation in the middle portion between A and B, one can see that a vortex and antivortex pair has formed in the opposite sides of the line joining A and B, see ref. [9] for details. These considerations can easily be generalized to other defects [9].

Numerical techniques used in this paper are the same as used in the earlier papers [8–10]. We study 2+1 dimensional case, with the Lagrangian taken as the following.

$$L = \frac{1}{2} \partial_\mu \Phi^\dagger \partial^\mu \Phi - \frac{1}{4} \phi^2 (\phi - 1)^2 + \epsilon \phi^3 + \kappa \phi^2 \cos \theta \quad (1)$$

This Lagrangian is written in terms of appropriately scaled coordinates, and a dimensionless complex scalar field  $\Phi$ , with  $\phi$  and  $\theta$  being the magnitude and the phase of  $\Phi$ . Value of  $\epsilon$  is taken to be 0.05. This Lagrangian describes a theory where U(1) global symmetry is spontaneously broken, except for the presence of last term which breaks U(1) explicitly.

For the case of  $\kappa = 0$ , the process of vortex creation via bubble nucleation has been studied in detail in ref. [16] for the Kibble mechanism, and in ref. [9,10] for the new mechanism. At zero temperature, the phase transition takes place via nucleation of bubbles of true vacuum in the background of false vacuum via quantum tunneling.

The bubble profile  $\phi$  is obtained by solving the Euclidean field equation [17]

$$\frac{d^2\phi}{dr^2} + \frac{2}{r} \frac{d\phi}{dr} - V'(\phi) = 0 \quad (2)$$

where  $V(\phi)$  is the effective potential in Eq.(1) (with  $\kappa = 0$ ) and  $r$  is the radial coordinate in the Euclidean space. In the Minkowski space initial profile for the bubble is obtained by putting  $t = 0$  in the solution of the above equation.  $\theta$  takes a constant value inside a given bubble.

The bubble profile found by solving Euclidean equation of motion Eq.(2) for  $\kappa = 0$  provides an adequate starting bubble configuration even for small non-zero values of  $\kappa$  as we are only interested in vortex formation which happens after bubbles expand and coalesce. This was the approach used in our earlier work [8] for the case with  $\kappa \neq 0$ . However, there is a nontrivial issue here. [This was pointed out to us by Copeland and Saffin]. The standard method of finding the bounce solution [17], for the present case with  $\kappa \neq 0$ , works fine if the phase  $\theta$  takes value 0 or  $\pi$  inside the bubble. For any other choice of  $\theta$ , the method does not work with the conventional approach. It appears that if at all there is any bounce solution for arbitrary  $\theta$ , it must require a non-uniform  $\theta$  inside the bubble [18].

For the purpose of the present paper, we will ignore this issue. One approach can be that if one was considering thermal nucleation of bubbles, then if the explicit symmetry breaking term is very small compared to the scale set by the temperature, then one can ignore it while considering the nucleation process itself. Thus we will continue to use the bubble profile obtained for the case of  $\kappa = 0$  and evolve the configuration with non-zero value of  $\kappa$ . The profile of the bubble calculated with  $\kappa = 0$  has the asymptotic value  $\phi = 0$  which is the local minimum of the effective potential. Hence it is suitable for nucleating the bubbles in the background of false vacuum,  $\phi = 0$ . This suggests that the explicit symmetry breaking term should be chosen such that the false vacuum remains the same  $\phi = 0$  so that there is no mismatch between the false vacuum and the asymptotic value of  $\Phi$  of different bubbles. The specific form of the explicit symmetry breaking term we use is motivated by this consideration as well as by simplicity. It is important to mention that our results are not sensitive to the form of the explicit symmetry breaking term, as long as the true vacuum (with non-zero value of  $\kappa$ ) is non-degenerate. We have verified that similar enhancement in vortex production results with other types of symmetry breaking terms as well, for example with  $\kappa\phi\cos\theta$ .

Even though we are neglecting the effects of explicit symmetry breaking in solving Eqn.(2) for the bubble profile, its effects should be taken into account when  $\theta$  inside bubbles is being determined ( $\theta$  inside a given bubble taken to be uniform). For  $\kappa = 0$  one takes all values of  $\theta$  to be equally probable. However, with  $\kappa \neq 0$  one will

expect a bias in  $\theta$  distribution inside bubbles as bubbles with smaller values of  $\theta$  will have smaller free energy and hence larger nucleation probability. We take into account this bias in  $\theta$  distribution inside bubbles later in Section IV. We show there that, in a simulation involving nucleation of 63 bubbles, bias in  $\theta$  distribution leads to all bubbles having  $\theta$  configurations such that not a single Kibble vortex/antivortex is produced. At the same time vortex production due to the new mechanism is essentially unaffected by the biased  $\theta$  distribution. However, in order to have a conservative estimate of the importance of the new mechanism compared to the Kibble mechanism, we first study situation where bubbles are nucleated with uniform probability of  $\theta$  for which Kibble mechanism contribution is well understood. This approximation will be consistent when the tilt is small compared to the temperature scale at which bubble nucleation is supposed to be happening. [Though, in that situation one should worry about validity of classical evolution using field equations as for large temperatures vortex-antivortex pairs can be thermally nucleated. We will consider this point later in Section IV. For now we will continue using uniform probability distribution for  $\theta$  inside bubbles.]

Rest of the numerical technique is the same as used in earlier works [8–10]. The field evolution is carried out using field equations obtained from Eqn.(1). The simulation of the phase transition is carried out by nucleating bubbles on a square lattice with periodic boundary conditions, i.e on a torus. Lattice spacing in spatial directions was taken to be  $\Delta x = 0.16$ , with time step  $\Delta t$  equal to  $\Delta x/\sqrt{2}$ . Simulations were carried out on an HP-735 workstation, a Silicon Graphics Indigo 2 workstation, and an HPK-260 workstation at the Institute of Physics, Bhubaneswar.

When evolved with these equations, bubbles grow, coalesce, and vortices are formed in the intersection region of three or more bubbles by Kibble Mechanism, as well as by the decay of bubble walls via the new mechanism. Note that, when  $\kappa$  is non zero then  $\theta = 0$  is energetically preferred (for our choice of explicit symmetry breaking term). So when a bubble with non-zero  $\theta$  is nucleated,  $\theta$  inside the bubble evolves towards  $\theta = 0$  and eventually starts oscillating about  $\theta = 0$  with decreasing amplitude. This non-trivial dynamics of  $\theta$  is one feature which makes the present case qualitatively different from the case of  $\kappa = 0$  considered in ref. [10]. We explain this in some detail in the following by considering a two bubble collision.

When two bubbles collide there is always  $\phi$  oscillations in the coalesced portion of the two bubbles. Magnitude of this oscillation depends on the  $\theta$  difference between the two bubbles as well as on the spatial separation between the two bubbles. As described in ref. [16],  $\phi$  oscillations are more prominent when  $\theta$  difference between the bubbles is small. Large  $\theta$  difference leads to large gradient energy in the coalesced region which suppresses  $\phi$  oscillations in that region. When  $\phi$  oscillations have sufficient amplitude then  $\Phi$  can overshoot the value  $\Phi = 0$

by climbing over the potential hill. Clearly, this leads to a change in  $\theta$  in that region to  $\theta + \pi$ , i.e. to flipping of  $\Phi$ . If this oscillation, and the associated flip, happens inside a region where  $\theta$  is spatially varying, then a pair of vortex-antivortex forms in this single flip (as explained at the beginning of this section). Note that so far in this picture we did not use anywhere the presence of explicit symmetry breaking (or, the rolling of  $\theta$  to zero). One will expect that every time this type of situation arises (even in the course of a single two bubble collision), it will lead to a vortex-antivortex pair getting nucleated. In fact, this is where the explicit symmetry breaking term in the effective potential plays a crucial role, as we describe below.

Consider two bubbles with associated values of  $\theta$  being  $\pi + \alpha$  and  $\pi - \alpha$  respectively, with  $\alpha < \pi/2$ . When these two bubbles collide, according to geodesic rule,  $\theta$  in the coalesced portion takes the value  $\theta = \pi$  (for this  $\alpha$  should be small as  $\theta$  rotates towards zero). Since  $\theta$  is rolling towards zero in both the bubbles we always encounter  $\theta = \pi$  as we go from one bubble to the other and there is a  $\theta$  gradient which keeps increasing due to rolling of  $\theta$ . It helps to think in terms of an arc spreading around the value  $\pi$  in the plot of the effective potential (see Fig.1) which represents the variation of  $\theta$  from the center of one bubble to the center of second bubble. Both ends of this arc (p and q) will roll down towards zero, and as the arc is constrained to go through the value  $\pi$  (due to continuity), it will lead to larger  $\theta$  gradients. Now if  $\Phi$  flips in this region due to  $\phi$  oscillation then we will get a vortex-antivortex pair. The vortex and the antivortex in this pair move away from each other as  $\theta$  is zero in between them while  $\theta$  in the outer directions is  $\pi$  having larger potential energy. This is how the first pair is created.

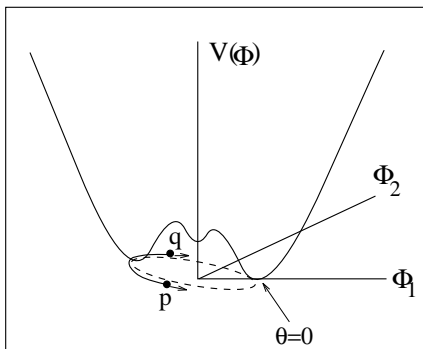


Fig. 1

FIG. 1. Plot of the effective potential.  $\theta$  variation in the physical space is taken to correspond to the solid arc. The end points, p and q, of the arc roll towards  $\theta = 0$ , but the arc is constrained to go through  $\theta = \pi$  due to continuity.

We note now that even though  $\theta$  is 0 in the coalesced portion, there is still a  $\theta$  gradient which arises due to  $\theta$

oscillation around zero in the bubbles. [ $\theta$  in each bubble, while rolling down towards 0, overshoots leading to non zero  $\theta$  gradient in that region.] If  $\phi$  oscillations are still strong enough so that they lead to yet another flip of  $\Phi$  then another vortex-antivortex pair will be nucleated. This process of successive pair creations continues till we have  $\theta$  oscillations maintaining  $\theta$  gradient in the coalesced portion and large  $\phi$  oscillations flipping  $\Phi$ . Creation of multiple pairs in this manner was demonstrated in ref. [8], where it was shown that as many as ten vortices and antivortices were created in a single, two bubble collision.

We have emphasized that if there is no flipping of  $\Phi$  then there will be no pair creation of vortices. Also, the amplitude of  $\phi$  oscillation in the coalesced region depends on the separation of bubbles, with larger separation leading to larger amplitude. This may lead one to think that if the bubbles are at the closest separation then there will be no large oscillation of  $\phi$  so there may not be any pair creation at all. This was indeed true for the case of  $\kappa = 0$  discussed in ref. [10]. However, this is not true for the present case, with  $\kappa \neq 0$ . Consider for example a configuration which leads to  $\theta = \pi$  in the coalesced region. The gradient energy density in  $\theta$  variation in the coalesced region will keep increasing as  $\theta$  in both the bubbles rolls towards 0. This, implies large energy in the coalesced portion due to explicit symmetry breaking term which can drive  $\phi$  to climb the potential hill and lead to the flipping of  $\Phi$ . [At least when  $\kappa$  is not too small, see below.] Therefore, there is at least one pair of vortex-antivortex pair nucleated for appropriate initial  $\theta$  even for smallest separation of the bubbles. As we will see later, even in the presence of strong damping one pair is still nucleated (in contrast to the case of ref. [10]), though successive nucleation may be suppressed depending on the magnitude of damping.

### III. SIMULATION OF THE PHASE TRANSITION

The preceding section explains how vortex-antivortex pairs are created in a two bubble collision in the presence of explicit symmetry breaking. It was shown in ref. [8] that a large number of vortex-antivortex pairs can form in a two bubble collision for appropriately chosen initial field configuration of bubbles. Clearly, in an actual phase transition, such large enhancement may not be expected due to randomness in values of  $\theta$  inside the bubbles as well as in their separations. This is especially so because the vortex production via this mechanism depends on the dynamical details of the bubble collisions and depends on parameters such as the magnitude of symmetry breaking term in the effective potential. Therefore, to find actual enhancement in the vortex production in this case one has to carry out the full simulation of the phase transition. We describe the results of such simulations in this section.

In this section we will present results with the value of  $\kappa = 0.015$ . Here, we will neglect the explicit symmetry

breaking term in determining  $\theta$  inside nucleated bubbles. In the next section we will take into account the effect of explicit symmetry breaking in biasing the  $\theta$  distribution. We will see that the average defect production per bubble, via the new mechanism, remains almost unaffected, while defect production via the Kibble mechanism becomes strongly suppressed for biased  $\theta$  distribution case.

Nucleation rate was suitably chosen so that there were all together seven bubbles nucleated in the whole lattice. Physical size of the lattice was taken to be  $192 \times 192$ . As we mentioned earlier, the location of bubbles in the lattice as well as the values of  $\theta$  inside them were chosen randomly. Number of bubbles was chosen to be small (by taking small nucleation rate) so that bubble collisions are energetic which helps in vortex-antivortex pair creation. Also the bubbles are nucleated only in a short time duration so they are roughly of same size when they collide. These bubbles then expand and coalesce.

Fig.2a shows the plot of  $\Phi$  at an early stage when bubbles have just started coalescing. [In all the plots of  $\Phi$ , the orientation of an arrow from the positive x axis corresponds to  $\theta$  and the length of the arrow is proportional to  $\phi$ .] Rotation of  $\theta$  can be clearly seen inside the bubbles. Due to  $\phi^2$  dependence in the  $\kappa$  term,  $\theta$  rotation is slowest near the bubble walls. Note that  $\theta$  in the central region of many bubbles has almost rotated to zero, the only memory of the initial values of  $\theta$  remaining near the walls. Interestingly, distribution of  $\theta$  at walls of different bubbles plays the most dominant role in the production of all the vortices observed in the simulations.

The location of the vortices was determined by using an algorithm to locate the winding number. As the phase transition nears completion via the coalescence of bubbles, magnitude of  $\Phi$  becomes non-zero in most of the region with well defined phase  $\theta$ . We divide each plaquette in terms of two (right angle) triangles and check, for each such triangle, whether a non-zero winding is enclosed. For this purpose we use the geodesic rule to determine  $\theta$  configuration in between two adjacent lattice points, see ref. [10] for details. Windings are detected only in regions where the magnitude of  $\Phi$  is not too small in a small neighborhood of the triangle under consideration. If  $\Phi$  is too close to zero in a region then that region is still mostly in the false vacuum and there is no stability for any windings present there. After getting *probable* locations of vortices using the above algorithm, we check the region containing each vortex/antivortex, using detailed phase plots and surface plots of  $\phi$  to check the winding of the vortex, and select only those vortices which have well defined structure. By checking similar plots at earlier as well as later time steps we determine whether the vortex was produced due to oscillation, and subsequent flipping, of  $\Phi$ , or via the Kibble mechanism.

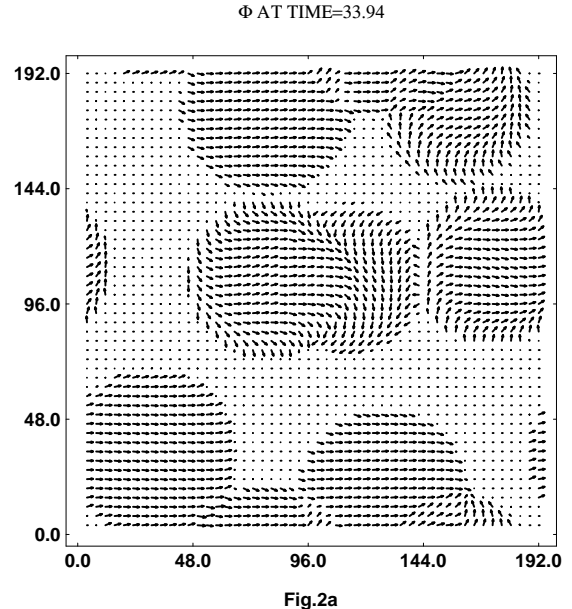


Fig.2a

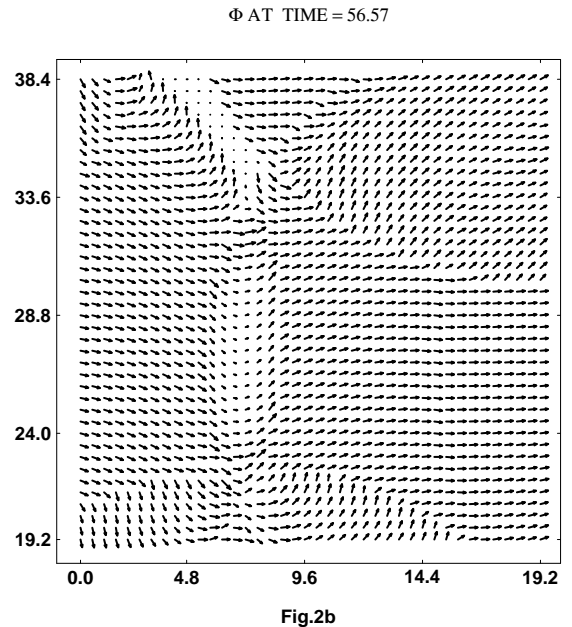


Fig.2b

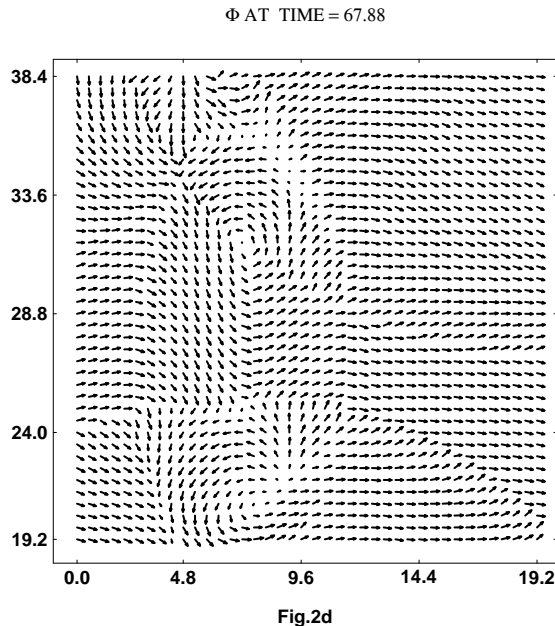
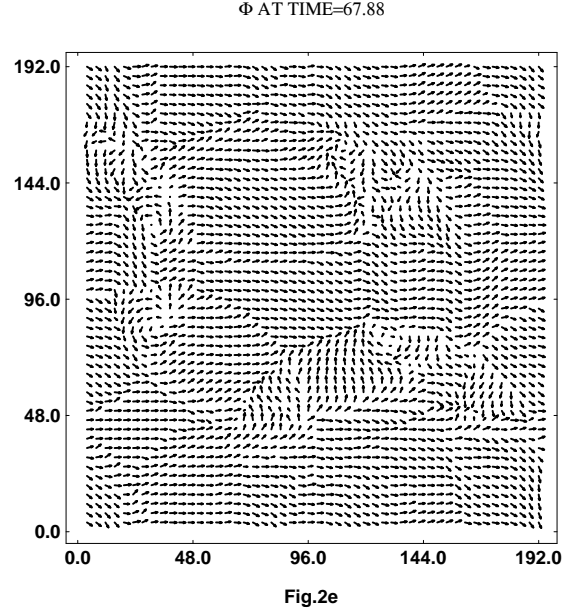
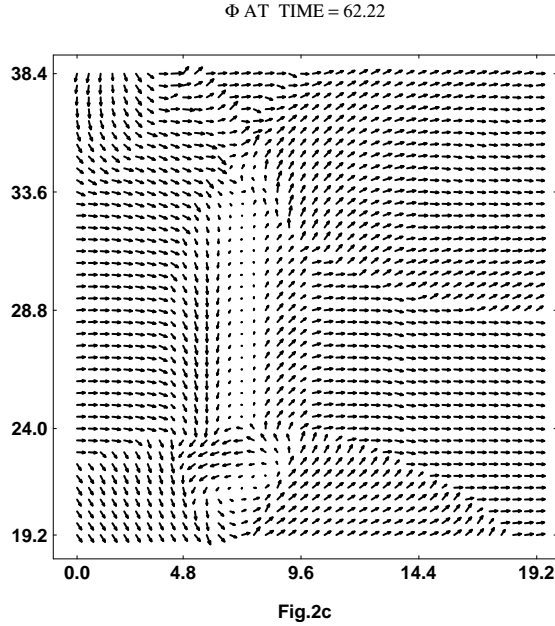


FIG. 2. (a) Plot of  $\Phi$  at an early stage when bubbles have just started coalescing. In all the plots of  $\Phi$ , the orientation of an arrow from the positive x axis corresponds to  $\theta$  and the length of the arrow is proportional to  $\phi$ . (b)  $\Phi$  plot in a region where there is no winding present at this stage. (c) An elongated region towards left of the center is oscillating, and a pair has been created. (d) Another pair has been created in this region due to continued oscillations. (e)  $\Phi$  plot of the entire lattice at a stage when maximum number of vortices and antivortices are present. Altogether, there are four vortex-antivortex pairs present at this stage.

Figs.2b, 2c and 2d show a region where two vortex-antivortex pairs form due to field oscillations. Fig.2b shows the plot of  $\Phi$  at  $t = 56.57$ . There is no winding present in the region at this stage. Fig.2c shows the plot at  $t = 62.22$ . We see that an elongated region towards left of the center is oscillating, and a pair has been created. These oscillations continue, leading to creation of another pair, as shown in Fig.2d. Fig.2e shows the  $\Phi$  plot of the entire lattice at this stage which corresponds to the situation when maximum number of vortices and antivortices are present. There are four vortex-antivortex pairs present at this stage. One of the pairs is near  $x = 36$ ,  $y = 96$ , second pair is near  $x = 36$ ,  $y = 132$ , third pair is near  $x = 136$ ,  $y = 72$ , and fourth pair is near  $x = 116$ ,  $y = 144$ .

In this particular simulation a total of (time integrated) 14 vortices and antivortices were formed. Out of these, only two are formed due to Kibble mechanism. This is consistent with the expected number density of  $1/4$  per bubble (for U(1) vortices in 2 spatial dimensions). Remaining twelve vortices and antivortices are formed

due to this new mechanism of coalesced bubble wall decaying by pair creation. This gives the average number of defects per bubble via the new mechanism to be about 1.7. Thus in this case this mechanism is completely dominant over the Kibble mechanism. Average number of all defects per bubble in this case is then 2.0 which is eight times larger than the number expected if vortices were only produced due to the Kibble mechanism. In all our simulations we have found strong enhancement of the number density of defects per bubble in the presence of explicit symmetry breaking. We should mention that apart from these 14 vortices and antivortices there were four additional pairs (i.e. eight vortices and antivortices) formed where vortices and antivortices were not well separated. Still windings of  $\theta$  corresponding to these pairs could be clearly seen in  $\theta$  plots. We do not count such pairs as these defects annihilate quickly. Such strongly overlapping pairs were found in all simulations.

There were some intriguing features observed in these simulations which we describe in the following. Fig.3a shows the field configuration at  $t = 42.42$ , where we see a well separated vortex-antivortex pair. The vortex and the antivortex move towards each other, as shown in Fig.3b. Due to asymmetric field configuration, the motion of the vortex-antivortex pair is not along the direction of their separation, rather the pair moves upward as a whole. The pair has annihilated by  $t = 50.91$ , as shown by the absence of any windings in Fig.3c. Subsequent plot at  $t = 53.74$  in Fig.3d shows that the vortex-antivortex pair has been re-created. Interestingly, however, this time the location of the vortex and the antivortex are reversed. It is as if the vortex and the antivortex have passed through each other. Also, by checking subsequent plots, we find that the motion of the pair as a whole is now downward. This new pair annihilates later. This pair, thus, represents a bound state of a vortex-antivortex system. There were several vortex-antivortex pairs for which this cycle of annihilation and re-creation was seen. In all the cases, the vortex and the antivortex were exchanged after first annihilation and re-creation. For some cases, the cycle was repeated, but when the pair was re-created second time, the vortex and the antivortex scattered back, instead of going through each other.

This process of the vortex and the antivortex passing through each other in the first cycle of annihilation and re-creation should be contrasted with the results in ref. [19,20] for vortex-antivortex scattering. For global defects it was argued in [19] that for vortex-antivortex collisions which are dominated by gradient energy considerations, the vortex and the antivortex should retrace their original paths (i.e. they should bounce back) in a process of annihilation in a head-on collision and subsequent re-creation. Numerical simulation of gauged vortices in [20] showed that in such collisions the vortex and the antivortex bounce back as long as their kinetic energies are not very large, but they go through each other for extremely energetic collisions. In light of these stud-

ies, our numerical results of passing through of vortex and antivortex suggests that the collision is sufficiently energetic that gradient energy considerations are not relevant any more, like the results in ref. [20] for large kinetic energies. An estimate of the velocities from Figs.3a and 3b shows the velocity of the vortex to be between 0.9 and 1 and that of the antivortex, between 0.8 and 1. The uncertainty in the velocity arises from the uncertainty in the locations of the centers of the vortices. These are indeed very large velocities. One would expect such large velocities to arise here due to the domain wall (arising due to the concentration of  $\theta$  gradient) stretching between the vortex and the antivortex. Scattering back of vortices in subsequent annihilations and re-creations is then understood as due to velocities of vortices being not too large, so the arguments of ref. [19] should be applicable. This scattering back of vortex-antivortex thus provides an illustration of the physical arguments given in ref. [19]. We mention here that vortex-antivortex annihilations were seen in  $\kappa = 0$  case also [10], but the vortex-antivortex pair was never re-created there. Presumably, the velocities at annihilation are much larger for the present case of  $\kappa \neq 0$ .

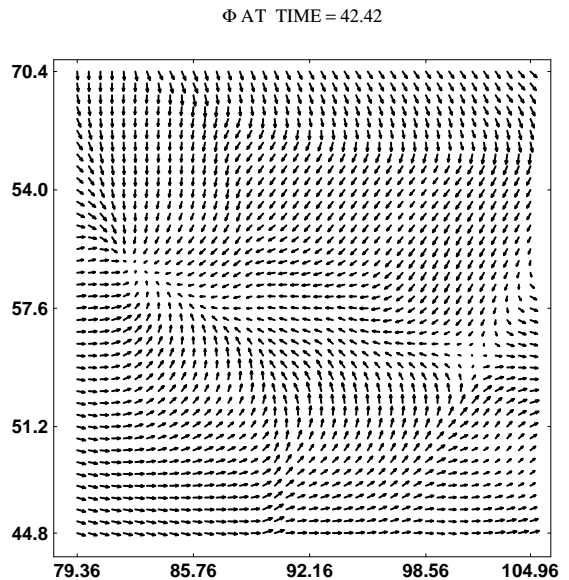


Fig.3a



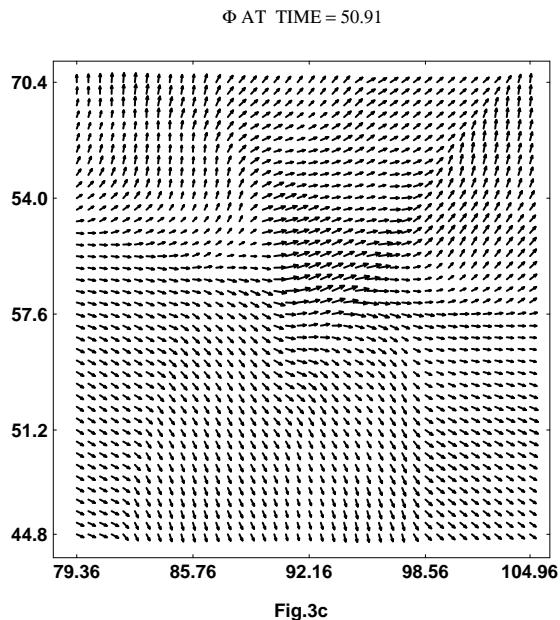
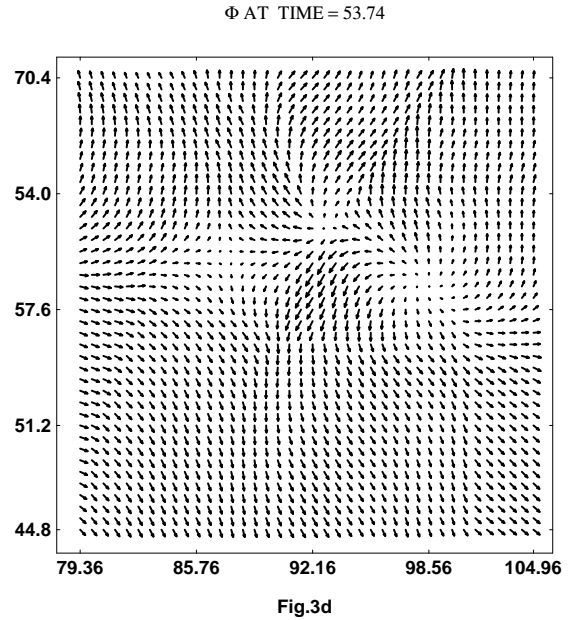
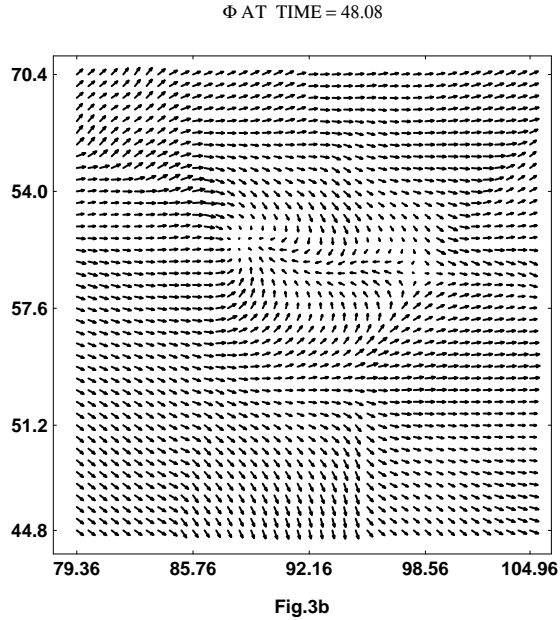


FIG. 3. (a) A well separated vortex-antivortex pair. (b) The vortex and the antivortex are moving towards each other, while the pair, as a whole, moves upwards. (c) Pair has annihilated by this time, as shown by the absence of any winding in this plot. (d) Vortex-antivortex pair has been re-created. Note that the positions of the vortex and the antivortex have been exchanged.

Another interesting result we find is for the cases of certain two bubble collisions which lead to vortex-antivortex pairs which are not well separated. However, due to presence of other bubbles, density waves arising from other bubble collisions propagate through the region where a given pair is getting formed. This density wave then strongly affects the  $\phi$  oscillations in that region and effectively separates the vortex and the antivortex. Thus, due to the effects of density wave, a pair which was strongly overlapping and was going to annihilate soon, ends up in well separated and well formed vortex and antivortex. This again shows that this new mechanism of pair creation strongly depends on the dynamical details of the transition. A density wave which as such can not contribute to defect production, leads to enhancement in the production of well separated defects. Similar effects were also found in ref. [10].

#### IV. DEFECT PRODUCTION WITH BIASED $\theta$ DISTRIBUTION

In this section we carry out a simulation as in Section III, but now with inclusion of a suppression factor in the nucleation rate for bubbles with a given  $\theta$  inside, resulting from the explicit symmetry breaking. As we will see, Kibble mechanism vortices get strongly suppressed. To get an idea of this suppression, we carry out a larger

simulation with nucleation of 63 bubbles, while average inter-bubble separation is the same as in Section III. This enables us to make direct comparison of average defect production per bubble for the two cases (as defect production via the new mechanism depends on average separation of bubble nucleation sites).

We estimate the suppression factor for bubble nucleation, with a given  $\theta$  inside, in the following manner. For this we assume that bubble nucleation is happening at some finite temperature  $T$ . (Even though the bubble profiles calculated in Section II correspond to  $T = 0$  case, we continue to use the same profiles. The reason for this is that we want to change only one factor here from the simulation of Section III, that is the  $\theta$  suppression factor. In any case, these are *thick wall* bubbles for which the profiles for  $T = 0$  and  $T \neq 0$  do not differ much. Also, actual profile of bubbles which is relevant for us is at the time when bubbles start coalescing. We are working with low nucleation rates, so bubbles expand by large amount before coalescing. Thus initial difference in the profiles becomes irrelevant.) This will lead to an additional factor  $\Gamma_\theta$  in the nucleation rate of the bubbles which arises due to the dependence of the effective potential on  $\theta$ . We have

$$\Gamma_\theta = e^{-F(\theta)/T} \quad (3)$$

where  $F(\theta)$  is the contribution to the free energy of the bubble arising from the explicit symmetry breaking term. For  $T$  we use the constraint that  $T$  should be less than typical energy required to create a vortex-antivortex pair, otherwise use of field equations for the evolution will become suspect. We thus estimate the energy of a pair of vortex-antivortex at various separations. For this we use a code for minimization of energy as was used in ref. [21]. To determine the energy of a vortex-antivortex pair, at a given separation, one starts with a trial profile for the pair. Field configuration is then fluctuated, while fixing the centers of the vortex and the antivortex, and energy is minimized. The configuration with the lowest value of energy is finally accepted as the correct profile of the vortex-antivortex pair and corresponding energy is taken as the energy of the pair. For details of the numerical technique, we refer the reader to ref. [21].

We find that at separation of about  $m_H^{-1}$  (between the centers of the vortices) the energy of the pair,  $E_{pair}$ , is about  $4.2 m_H$ , while at separation of  $2m_H^{-1}$  and  $3m_H^{-1}$ ,  $E_{pair}$  increases to about  $5.8 m_H$  and  $6.0 m_H$  respectively. For the consistency of using field equations for the evolution, we require  $T < E_{pair}$ . To get  $F(\theta)$ , we integrate the explicit symmetry breaking term in Eqn.(1) for the profile of the bubble (determined from solving Eqn.(2)). We find  $F(\theta) \simeq -3.6 m_H \cos\theta$ . We choose a sample value of  $T$  (satisfying the constraint that  $T < E_{pair}$ ) as  $T \simeq 1.8 m_H$ . Resulting value of  $F(\theta)/T$  is then simply equal to  $-2.0 \cos\theta$ . With this, we use the following (suitably normalized) expression for  $\Gamma_\theta$  for determining bias in  $\theta$  distribution in bubble nucleations.

$$\Gamma_\theta = e^{2(\cos\theta-1)} \quad (4)$$

With this choice of normalization,  $\Gamma_\theta$  is 1 for  $\theta = 0$  and is lowest, equal to  $e^{-4}$ , for  $\theta = \pi$ .

We then nucleate bubbles, with inclusion of this factor for  $\theta$  suppression. To have reasonable statistics (due to strong suppression of Kibble vortices in this case) we carry out simulation over a larger physical region with size equal to  $576 \times 576$ . Total number of bubbles nucleated was 63 which lead to about the same average bubble separation as in Section III. Just as in Section III, bubble locations are determined randomly, but now  $\theta$  inside bubbles is chosen with the weight factor  $\Gamma_\theta$  as give in Eqn.(4).

Resulting  $\theta$  distribution of the bubbles is shown in Fig.4. Solid dots show the frequencies  $P(\theta)$  of different values of  $\theta$  obtained in the simulation, normalized so that the maximum value of  $P(\theta)$  is 1.0. Solid curve is the plot of  $\Gamma_\theta$ . Most important thing to note in Fig.4 is an almost complete absence of  $\theta$  points in the range  $3\pi/2 > \theta > \pi/2$ . In fact, there were three bubbles with  $\theta$  being slightly less than  $3\pi/2$ , or slightly more than  $\pi/2$ . However, we verified that very quickly, during the evolution and much before any other bubble collides with these,  $\theta$  in these bubbles rotates (due to explicit symmetry breaking) and also falls in the range  $3\pi/2 < \theta < \pi/2$ . It is then immediately obvious that there is no possibility of any Kibble mechanism vortex forming by coalescence of these bubbles as no winding can be generated by following the geodesic rule. We have also verified it explicitly, by considering detailed field configurations of the vortices.

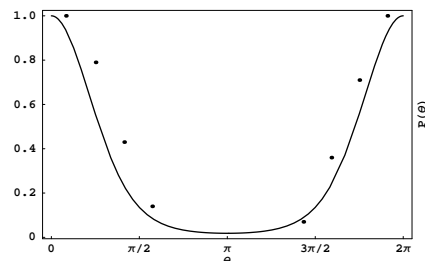


FIG. 4.  $\theta$  distribution inside bubbles. Dots show the normalized frequency  $P(\theta)$  of  $\theta$  inside different bubbles nucleated in the simulation. Solid curve is the plot of  $\Gamma_\theta$ .

We get a total of 52 vortex-antivortex pairs (i.e. 104 vortices and antivortices), all due to the new mechanism. This gives the average defect production per bubble to be about 1.65 which is essentially the same as the average number of defects per bubble via the new mechanism, as found in the simulation in Section III. Thus biased  $\theta$  distribution does not seem to adversely affect defect production via this new mechanism. This results is important

as it shows that in certain situations, with explicit symmetry breaking, this mechanism may not just dominate, it may be the only mechanism active for defect production. Effect of biased  $\theta$  distribution on this mechanism can be understood as follows. Suppression of larger values of  $\theta$  leads to smaller potential energy being stored in the collision regions, and this should adversely affect wall oscillation and hence defect production. However, now average  $\theta$  difference between coalescing bubbles will be smaller. As mentioned earlier, this helps in increasing wall oscillations, as less energy is spent in overcoming  $\theta$  gradients. This should lead to increase in defect production. Final defect production will be a combination of both these factors.

In next sections, we will study effects of changing nucleation rate, magnitude of explicit symmetry breaking, and presence of damping, on defect production via this new mechanism. As  $\theta$  suppression does not seem to affect this mechanism much, we will not include its effect in these sections. This also helps in making conservative comparison of this mechanism with the Kibble mechanism, when these parameters are varied, as in absence of any bias in  $\theta$  distribution Kibble vortices are also suppressed.

## V. DEPENDENCE OF DEFECT PRODUCTION ON NUCLEATION RATE AND $\kappa$

The results discussed in last two sections show that there is a strong enhancement in the number of defects produced in a phase transition due to this new mechanism. In this section we will study the dependence of this enhancement in defect production on the magnitude of symmetry breaking coefficient  $\kappa$  and on the nucleation rate. We start by discussing the effects of changing the nucleation rate, which in effect changes the average separation between bubbles.

We use  $\kappa = 0.015$  as in Section III, and keep it fixed while we carry out simulations with different values of the nucleation probability. As we are now using uniform probability for  $\theta$  distribution inside bubbles, we will compare the results of this section with those in Section III. Bubble nucleation probability used for the case discussed in Section III lead to seven bubbles nucleated in the lattice. We have studied two other cases by changing the nucleation probability. In one case the net number of bubbles nucleated was 12 and in the other case number of bubbles was 20.

For the case of 12 bubbles we found a total of 18 vortices. Out of these, 3 pairs of vortex-antivortex formed a cluster. For this simulation the total defect density per bubble comes out to be 1.5 which is less than the case of seven bubbles discussed in the previous section. This is consistent with the physical picture of this mechanism we discussed earlier where we mentioned that energetic bubble collisions will lead to larger oscillations of  $\phi$  in the coalesced portions of bubble walls and consequently

to larger number of vortex-antivortex pairs getting produced. Twelve bubble case leads to smaller value of average separation between bubbles compared to the seven bubble case and hence less energy for  $\phi$  oscillations.

As for the case of seven bubbles of Section III, here also we find several additional pairs of vortex-antivortex which correspond to strongly overlapping vortex-antivortex configurations. These did not separate and lasted only for a short time. There were three such pairs in the present case of twelve bubbles but we did not count them in the total number of vortices.

For the second case we take the value of nucleation probability so that there are twenty bubbles nucleated in the whole lattice. Since the average separation between the bubbles is smallest in this case compared to the previous two cases, the field oscillations flipping  $\Phi$  will be weakest in this case. Thus we expect that the pair production mechanism will not lead to many defects in this case. This is precisely what we find as the total number of vortices and antivortices in this case comes out to be 14. This gives the number density of all defects per bubble to be equal to 0.7. Again, apart from these 14 defects, we found six vortex-antivortex pairs which are strongly overlapping and therefore are not counted in determining the net number of defects. These results are similar to those found in ref. [10] where larger nucleation rate lead to a smaller number of well separated pairs being produced.

To study the effect of  $\kappa$  on the number density of defects we took the initial field configuration to be that corresponding to the case of twelve bubbles mentioned above. We then carry out simulations for various values of  $\kappa$ , each time starting with exactly the same initial field configuration. It is easy to see that increasing  $\kappa$  will lead to faster rolling of  $\theta$  inside the bubbles. From this one may have the impression that larger values of  $\kappa$  may lead to smaller number of defects as  $\theta$  will be close to zero in all the bubbles. As mentioned in ref. [8], this indeed does happen for values of  $\kappa$  which are so large that  $\theta$  in the bubbles settles down to zero before the  $\phi$  oscillations can take place. For our choices of parameters in Eqn.(3), this happens for values of  $\kappa$  larger than 0.03, see ref. [8].

However, as long as  $\kappa$  is smaller than this value, an increase in its value leads to increase in the defect production. It is easy to understand why this happens. Increasing  $\kappa$  leads to increase in the potential energy, as well as the gradient energy of the field configuration in the coalesced region. For example, the region where  $\theta$  takes value  $\pi$  has much larger energy with larger value of  $\kappa$ . There is, thus, more energy available for wall to decay in vortex-antivortex pairs leading to larger number of defects.

The case of twelve bubbles which we described above corresponded to the value of  $\kappa$  equal to 0.015. We repeated that simulation (with exactly same initial field configuration) for two other values of  $\kappa$ , one with  $\kappa$  equal to 0.01 and the other with  $\kappa$  equal to 0.02. For the case with  $\kappa$  equal to 0.01 we got a total of 12 vortices and an-

tivortices giving the average number of defects per bubble to be 1.0. This should be compared with the defect density per bubble = 1.5 for  $\kappa = 0.015$  case. From the above discussion, this decrease in defect production for smaller value of  $\kappa$  is expected. For  $\kappa = 0.02$  we found a total of 22 vortices and antivortices giving the density of defects per bubble to be equal to 1.8, clearly a significant increase. In this series of simulations for different values of  $\kappa$  we found that some of the two bubble collisions lead to vortex-antivortex pairs only for  $\kappa = 0.02$ . (Note that initial bubble configurations have been chosen to be identical for all the three cases.) Which implies that  $\phi$  oscillations were large enough to flip  $\Phi$  only for this larger value of  $\kappa$ .

There is one important feature we found which needs to be emphasized. In the case of  $\kappa = 0.01$  (for twelve bubble case), we found that out of the total of 12 vortices, eight vortices can be attributed to be forming from the Kibble Mechanism and four from the pair production process. However, when the simulation was repeated for  $\kappa = 0.0$  (again starting with exactly same initial field configuration) then only four vortices formed via the Kibble mechanism. The reason that the vortices corresponding to the Kibble mechanism are fewer in this case is that these corresponded to collisions of more than three bubbles. Altogether these bubbles had zero net winding but taken in groups of three bubbles at a time, they had winding and anti-winding (using the geodesic rule). In the case of  $\kappa = 0.0$  this vortex and antivortex immediately annihilate each other (or in some sense their windings annihilate each other even before they could form). However, for non-zero  $\kappa$ , this vortex and antivortex get separated in order to minimize the energy as  $\theta$  in between the vortex and antivortex takes the value zero which is the absolute minimum of the effective potential. Thus explicit symmetry breaking, in addition to producing defects via wall decaying into pairs, also can enhance the defect production via the Kibble mechanism in certain situations.

To summarize the results of this section, we found that increasing the nucleation rate decreases the number density of vortices per bubble which is due to decrease in average separation between the bubbles. Smaller separation between bubbles leads to a suppression in  $\phi$  oscillations and consequently decreases the defect production. Increase in the magnitude of the explicit symmetry breaking  $\kappa$ , increases the number density of vortices per bubble. This is attributed to enhancement in  $\phi$  oscillation coming from the increase in potential energy and gradient energy of wall configuration in the coalesced region due to a larger  $\kappa$ .

## V. EFFECT OF DAMPING ON THE NEW MECHANISM

So far our discussion (as well as the discussion in ref. [8]) was for the case with no dissipation present. Since

the creation of vortex-antivortex pairs via this mechanism crucially depends on  $\phi$  oscillations (and on  $\theta$  gradient which comes from  $\theta$  oscillations), it is natural to expect that the presence of damping can crucially affect the effectiveness of this mechanism. It is thus important to understand the precise manner in which damping affects this mechanism. After all, damping is naturally present in most cases of interest, such as the early Universe, liquid crystal systems and even quark-gluon plasma at finite temperature (for the case of Skyrmions).

In this section we will present results of simulations of two bubble collisions in presence of dissipation and study how the defect production is affected. What we expect to find is that the presence of damping should suppress the defect production via this mechanism. This is because damping will lead to suppression in the amplitudes of successive oscillations of  $\phi$  in the wall so that it will become difficult for  $\Phi$  to flip. Consequently, production of vortex-antivortex pairs will be suppressed. This is what we find in our simulations, which we describe in the following.

We have studied the effect of damping on the creation of vortices in two bubble collision by introducing a damping term  $\eta\dot{\phi}$  in the equation of motions for evolving the field configuration. Lattice size is taken to be  $160 \times 128$ , with the same lattice spacing as before. We choose the initial field configuration of the two bubbles to be the one which leads to formation of three vortex-antivortex pairs when damping is absent. Value of  $\kappa$  is taken to be equal to 0.015. We then repeat the simulation for this two bubble collision starting with exactly the same initial configuration, but now in the presence of damping. We study the effect of magnitude of damping by changing the damping coefficient  $\eta$ . In the presence of damping, bubble wall velocity is smaller so the bubble collision is less energetic to begin with. Further, as the oscillating  $\phi$  in the coalesced region loses energy also due to damping, successive oscillations are strongly suppressed. This leads to suppression in the number of pairs getting formed.

For small values of  $\eta$  (in the range 0.0 to 0.25) we still get three vortex-antivortex pairs. But for the values of  $\eta$  larger than 0.25,  $\phi$  oscillations are strongly suppressed and only one pair is formed. For  $\eta = 1.0$ , even the one pair formed corresponds to a vortex and an antivortex which are very close to the wall of the coalesced bubbles and are not well formed.  $\phi$  oscillations are very strongly suppressed in this case and  $\theta$  almost settles down to zero without any oscillation about  $\theta = 0.0$ . Figs.5a and 5b show surface plots of  $-\phi$  of the coalesced region of the two bubbles, at the same stage,  $t = 84.85$ , for the two cases,  $\eta = 0.1$  and  $\eta = 0.75$  respectively. Starting  $\theta$  in both the bubbles was such that  $\theta$  in between the bubbles interpolates through  $\theta = \pi$ . As we mentioned above, the initial field configurations of the two bubbles were identical for both of these cases. We see that there are two, well formed, vortex-antivortex pairs present in Fig.5a, for  $\eta = 0.1$  case. In contrast, at the same stage, there is only one pair present in Fig.5b for  $\eta = 0.75$  case. For  $\eta = 0.1$

case, one more pair forms later, making total number of pairs formed equal to 3 for this case. However, by that time, the only pair formed for the  $\eta = 0.75$  case escapes out of the walls of the coalesced bubble (due to  $\theta$  being zero between the pair, and  $\theta = \pi$  in directions towards the walls), hence we do not show plots at that stage.

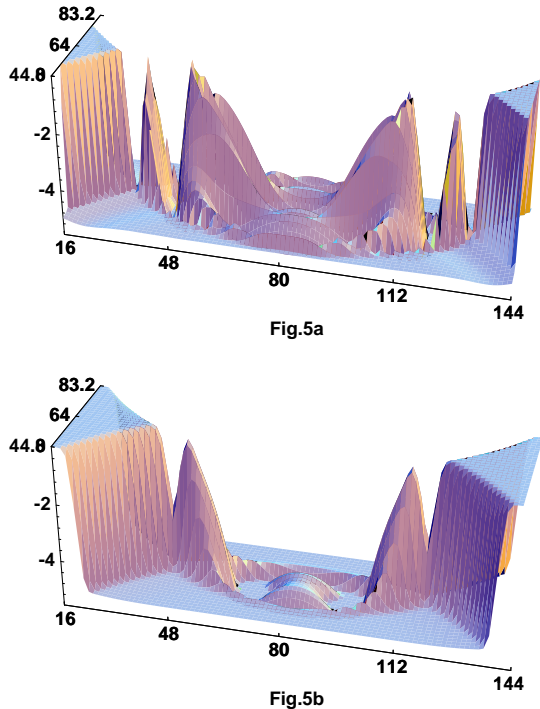


FIG. 5. (a) Surface plot of  $-\phi$  for  $\eta = 0.1$  of the coalesced region of two bubbles, showing profiles of two vortex-antivortex pairs. One more pair forms later in this case. (b) Surface plot of  $-\phi$  for  $\eta = 0.75$  showing the profile of the single pair formed in this case. Later, this vortex and the antivortex escape out of the coalesced bubble. Both these plots are shown at the same time stage,  $t = 84.85$ , starting with identical initial field configurations of the two bubbles.

We emphasize here that whatever be the value of the damping coefficient, there is always at least one vortex-antivortex pair formed with favorable initial configuration of two bubbles (i.e.  $\theta$  distribution) via the new mechanism. This happens because the potential energy contained in the coalesced region will make the flipping of  $\Phi$  (and hence the pair production) favorable compared to rolling down of the two ends of the arc in Fig.1 as that leads to constantly increasing gradient energy. We also mention that irrespective of damping (or even the order of phase transition) one pair should always form, for appropriate values of  $\theta$  in the two bubbles, via the mechanism discussed in ref. [13] as  $\phi$  oscillations play no role there. However, we have checked that rotation of  $\theta$  in the walls is so slow (due to the presence of  $\phi^2$  in the explicit symmetry breaking term) that one will expect the pair formation via the mechanism of ref. [13] only after a very

long time. On the other hand, pair formation due to  $\phi$  flipping happens in a much shorter time scale, that of a single  $\phi$  oscillation in the wall.

Another important point which should be mentioned here is that, in the presence of strong damping, no pair may get created if  $\kappa$  is too small. In the presence of strong damping one can neglect the kinetic energy of the bubble wall. So what remains is the contribution from the explicit symmetry breaking term, which must lead to the flipping of  $\Phi$  by forcing it to go through zero. However, below a certain critical value of  $\kappa$  it may not happen, as the  $\theta$  gradient developed in the coalesced portion of the bubbles may form a stable domain wall. This will be like the axionic domain wall [14], which can decay only via quantum tunneling (say, at zero temperature).

This is an appropriate point to discuss an important issue about the applicability of the new mechanism for different types of defects. There is one class of defects where the applicability of this mechanism may hold only in some special situations, and not generically. These correspond to vacuum manifolds for which the opposite orientations of the order parameter field are identified. Nematic liquid crystals happens to belong to this category, with the vacuum manifold being  $RP^2$ . In such cases, flipping of the order parameter field does not change its configuration. Thus the argument given above for the pair production can not be directly applied here. However, it is possible to argue that in the presence of explicit symmetry breaking this mechanism should still be applicable, especially when the system is dissipative. Consider, for example, an order parameter configuration varying around a point P in the physical space smoothly such that the value of the order parameter at P is energetically most unfavorable (due to explicit symmetry breaking). For the case described by Eqn.(1) it means  $\theta$  having value  $\pi$  at point P, and varying from a value less than  $\pi$  to a value larger than  $\pi$  as we cross P in the physical space.

For nematic liquid crystals, say, in the presence of external electric field along the x axis, it means that the director (order parameter) will lie in the y-z plane at the point P, and will deviate from the y-z plane in opposite directions as one passes through P in the physical space. As the order parameter field rolls down to the direction of the true vacuum, a region of large gradient energy will arise near P. As we explained above, for sufficiently small explicit symmetry breaking, the gradient energy may not become too large, and may result in the formation of a domain wall in that region. However, for larger values of explicit symmetry breaking (e.g., stronger electric field for the liquid crystal case), the gradient energy will keep rising, eventually forcing the field to go to zero magnitude in the region near P. The only way to decrease the energy of this configuration is by creating a defect-antidefect pair. For extremely damped situations it may happen gradually as the director reaches zero magnitude at P and then slowly grows in magnitude but now with an orientation along the x axis, thereby

resulting in the creation of vortex-antivortex pair (for 2-dimensions, and a loop of string for 3-dimensions). For smaller damping, or for that matter, in the absence of damping, the order parameter field may keep oscillating at  $P$  through zero, without changing its configuration in passing through zero. During the passage of the field through zero, any small fluctuation can re-orient the director along the  $x$  axis, resulting in the pair production. Or, the field may eventually settle at zero (either due to the damping term, or just due to loss of energy in successive oscillations in other excitations of the system), and then *roll down* to a direction along the  $x$  axis. This will then again result in the pair production via this mechanism. In the absence of any explicit symmetry breaking, this mechanism does not seem to be applicable for these types of vacuum manifolds.

## VI. CONCLUSIONS

We conclude by emphasizing the essential aspects of our results. We have carried out numerical simulations of a first order phase transition by random nucleation of bubbles, in the presence of small explicit symmetry breaking, and have studied the production of vortices and antivortices. We estimate the net number density (number of defects per bubble) of vortices produced, which includes vortices formed due to the Kibble mechanism as well as those produced via the pair production mechanism. We also study the dependence of this defect number density on parameters such as the magnitude of the explicit symmetry breaking term as well as on the nucleation rate. Defect production increases with larger magnitude of explicit symmetry breaking due to larger potential energy in the coalesced region. Nucleation rate affects defect density due to the fact that a larger nucleation rate implies smaller average bubble separation, which in turn leads to less kinetic energy for the bubble walls before bubbles collide. Oscillations of  $\phi$  are less prominent for less energetic walls leading to smaller number of defects for larger nucleation rates. We have also studied the effects of presence of damping on this pair production mechanism by studying pair production in two bubble collisions. As expected, we find the damping suppresses oscillations of  $\phi$  and hence leads to smaller number of defects, though one pair is always produced (for suitable values of  $\theta$  distribution in the bubbles, and for  $\kappa$  not too small).

In all these cases we find that the number of defects produced due to effects of explicit symmetry breaking term (either via direct pair production mechanism, or by separating vortex-antivortex pairs produced in collisions of more than three bubbles via the Kibble mechanism) is much larger than what one would expect from the Kibble mechanism. This relative enhancement is much larger when we include the effect of bias in  $\theta$  distribution in bubbles, resulting from explicit symmetry breaking. In this case we find, in a simulation with 63 bubbles, that

not even a single defect is produced via the Kibble mechanism, while 104 vortices and antivortices are produced via the new mechanism. As the distribution of these defects is of very different nature than the one expected from the Kibble mechanism, one may expect qualitatively new features for systems with explicit symmetry breaking. In our 2+1 dimensional study we find a sequence of vortex-antivortex pairs being produced. Simple arguments show that for 3+1 dimensions one will get a system of concentric string loops, (see ref. [8] for example). This may then suppress formation of large strings compared to small loops. It will be of great interest if such a prediction can be experimentally verified in some physical system. As mentioned in ref. [8], formation of strings in nematic liquid crystals in the presence of external electric or magnetic fields may be ideal for checking this mechanism. (Though in that case, presence of damping may suppress string formation via this new mechanism.)

## ACKNOWLEDGMENTS

We are very grateful to Ed Copeland and Paul Saffin for very useful comments, especially for pointing out to us the non-trivial issue of correct bounce solution for the case with explicit symmetry breaking. We also thank an anonymous referee for useful comments about constraints on temperature for bubble nucleation in presence of explicit symmetry breaking, and about  $\theta$  suppression factor in bubble nucleation.

- 
- [1] For a review see, A. Vilenkin and E.P.S. Shellard, "Cosmic strings and other topological defects", (Cambridge University Press, Cambridge, 1994).
  - [2] F.A. Bais and S. Rudaz, Nucl. Phys. **B170**, 507 (1980); F. Liu, M. Mondello, and N. Goldenfeld, Phys. Rev. Lett. **66**, 3071 (1991).
  - [3] T.W.B. Kibble, J. Phys. **A9**, 1387 (1976).
  - [4] For a review, see, W.H. Zurek, Phys. Rep. **276**, 177 (1996).
  - [5] S. Digal, R. Ray, and A.M. Srivastava, hep-ph/9805502.
  - [6] E.J. Copeland and P.M. Saffin, Phys. Rev. **D54**, 6088 (1996).
  - [7] J. Borrill, T.W.B. Kibble, T. Vachaspati, and A. Vilenkin, Phys. Rev. **D52**, 1934 (1995).
  - [8] S. Digal and A.M. Srivastava, Phys. Rev. Lett. **76**, 583 (1996).
  - [9] S. Digal, S. Sengupta, and A.M. Srivastava, Phys. Rev. **D55**, 3824 (1997).
  - [10] S. Digal, S. Sengupta, and A.M. Srivastava, Phys. Rev. **D56**, 2035 (1997).
  - [11] E.J. Copeland and P.M. Saffin, Phys. Rev. **D56**, 1215 (1997).
  - [12] G.E. Volovik, Czech. J. Phys. **46**, 3048 (1996) Suppl. S6;

- T.D.C. Bevan, A.J. Manninen, J.B. Cook, J.R. Hook, H.E. Hall, T. Vachaspati, and G.E. Volovik, *Nature*, **386**, 689 (1997).
- [13] J.I. Kapusta and A.M. Srivastava, *Phys. Rev.* **D52**, 2977 (1995).
- [14] For a detailed discussion see, E.W. Kolb and M.S. Turner, “The early Universe”, (Addison-Wesley, Redwood City, California, 1990).
- [15] P. G. de Gennes, “The physics of liquid crystals”, (Clarendon, Oxford, 1974).
- [16] A.M. Srivastava, *Phys. Rev.* **D45**, R3304 (1992); **D46**, 1353 (1992); S. Chakravarty and A.M. Srivastava, *Nucl. Phys.* **B406**, 795 (1993).
- [17] M.B. Voloshin, I.Yu. Kobzarev and L.B. Okun, *Yad. Fiz.* **20**, 1229 (1974) [*Sov. J. Nucl. Phys.* **20**, 644 (1975)]; S. Coleman, *Phys. Rev.* **D15**, 2929 (1977).
- [18] E.J. Copeland and P.M. Saffin, private communication.
- [19] C. Rosenzweig and A.M. Srivastava, *Phys. Rev.* **D 43**, 4029 (1991).
- [20] K.J.M. Moriarty, E. Myers and C. Rebbi, *Phys. Lett.* **B207**, 411 (1988).
- [21] A.M. Srivastava, *Phys. Rev.* **D 47**, 1324 (1993).

This figure "fig1-1.png" is available in "png" format from:

<http://arxiv.org/ps/hep-ph/9707221v2>



This figure "fig1-2.png" is available in "png" format from:

<http://arxiv.org/ps/hep-ph/9707221v2>

This figure "fig1-3.png" is available in "png" format from:

<http://arxiv.org/ps/hep-ph/9707221v2>

This figure "fig1-4.png" is available in "png" format from:

<http://arxiv.org/ps/hep-ph/9707221v2>

This figure "fig1-5.png" is available in "png" format from:

<http://arxiv.org/ps/hep-ph/9707221v2>

This figure "fig1-6.png" is available in "png" format from:

<http://arxiv.org/ps/hep-ph/9707221v2>

This figure "fig1-7.png" is available in "png" format from:

<http://arxiv.org/ps/hep-ph/9707221v2>

This figure "fig1-8.png" is available in "png" format from:

<http://arxiv.org/ps/hep-ph/9707221v2>

This figure "fig1-9.png" is available in "png" format from:

<http://arxiv.org/ps/hep-ph/9707221v2>



This figure "fig1-10.png" is available in "png" format from:

<http://arxiv.org/ps/hep-ph/9707221v2>

This figure "fig1-11.png" is available in "png" format from:

<http://arxiv.org/ps/hep-ph/9707221v2>

This figure "fig1-12.png" is available in "png" format from:

<http://arxiv.org/ps/hep-ph/9707221v2>